Chapter 3

Evaluation of a free convection corrugated type of solar dryer for Garcinia pedunculata: An investigation on kinetics, energy, and economic aspects

Increase in population in the North East region of India implies to save the indigenous fruits with tremendous health benefits and *Garcinia pedunculata* (GP) is one such product that needs great attention. GP has immense medicinal characteristics but often ignored because of the seasonality of the fruit. The tree starts bearing flowers by September-October and ripens in April. The monsoon dominates at this time of the year and it is very difficult to dry products in such adverse condition. Along with it, the uncertainty of climatic condition all across the world has created unexpected problems for the farmers as well as consumers. *Garcinia pedunculata* is an advantageous fruit which when not stored properly may lead to contamination. Being a medicinal fruit, GP improves digestion, cleanses urine, serves as a heart tonic, eases constipation, and cures abdominal tumours, worm infestation, digestive problems, vomiting, hemorrhoids, and several other ailments [64–66]. As such drying of seasonal medicinal fruits is supremely important for availing them throughout the year. Therefore, a novel free convection corrugated solar dryer (FCCSD) was developed for drying *Garcinia pedunculata* suitable for north-eastern region of India. This FCCSD is expected to give better quality dried products in lesser time for enhanced income generation of some rural farmers. The thin layer drying kinetics studies of GP dried under the open sun as well as in FCCSD with a mathematical modelling were performed. The payback period of the developed dryer was also estimated.

3.1 Description of free convection corrugated type of solar dryer

The solar air heater was free convection type with a corrugated absorber plate. The five sides of the air heater were made of 19 mm thick ply boards. The inner walls of the dryer were fixed with 1mm thick stainless-steel sheet. This was done to facilitate better heat reflection back into the dryer. The dimension of the solar air heater was 1800 mm×800 mm×150 mm. A glass sheet of a thickness of 4 mm was used as a cover to trap solar radiation. The corrugated absorber plate was painted black and this had dimension of 1600 mm×800 mm×1 mm. The entry and outflow paths of the ambient air are shown in Figure 3.1. Three long aluminium perforated trays of dimension 1570 mm×150 mm were

positioned above the corrugated solar air heater. Hence a prototype of FCCSD consisting of the corrugated absorber plate, a perforated long tray was designed and fabricated. The layout is shown in Figure 3.1 and a photo of the dryer loaded with *Garcinia pedunculata* is shown in Figure 3.2 respectively. FCCSD was experimentally tested in two batches and compared with open sun drying (OSD) and the average velocity of air was found to be 0.1 ms^{-1} and air flow rate of 0.00735 kgs^{-1}.

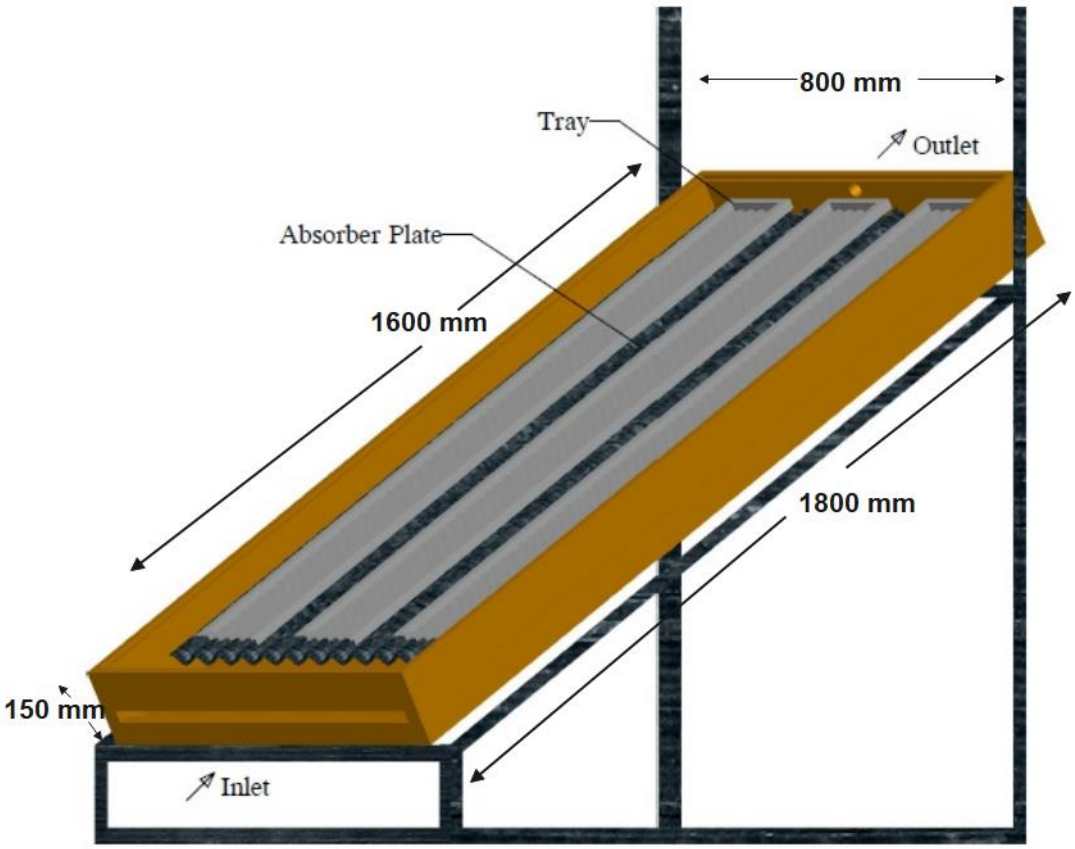

Figure 3.1 Prototype of direct type free convection corrugated solar dryer

Figure 3.2 Photograph of FCCSD loaded with GP

3.2 Experimental procedure

In Assam, India, the traditional method of drying GP involves using sunlight, which has several disadvantages. These include the build-up of dirt, infestation by pests, bacterial contamination, and damage from rain, rendering the dried items unhygienic and unsuitable for human consumption. However, with the development of an enhanced solar dryer for GP drying, it is anticipated that the process will yield consistent, high-quality products. This advancement will also lead to increased value addition and income generation for local farmers in rural areas. Fifteen kilogram of the freshly harvested GP was collected from the local market in April 2019, weighed and stored in a refrigerator (-30 °C) in airtight containers to test. The test was conducted for two batches, one from 12th to 14th October 2019 and another from 16th to 18th October 2019. For each batch, GP was taken out of the refrigerator and brought to room temperature. GP was cleaned with water to remove dirt from the surface. Each GP was then sliced into samples of 4 mm thick and uniformly distributed on perforated trays. 100 g of sliced GP in each tray was first taken as a sample and the rate of removal of moisture was measured. Another 2 kg sample was directly placed under the sun. The duration of experimenting was set for seven h per day (9:30 h to 16:30 h) for three days in open sun drying for both the batches. Each day as soon as the experiment was concluded, the dried products were stored in airtight containers. At different positions

of the dryer, the temperatures and relative humidity were recorded. The mass flow rate, the velocity of the air and solar radiation intensity were also noted. The mass loss of the GP sample was recorded at every 1 h interval employing a digital balance. The temperature of the air at various positions of the unit was measured using K-type thermocouples [accuracy ± 0.1 °C]. The relative humidity and the velocity of air were found with Anemometer with RH count Probe [Model: HTC AVM-06, range 0.1-30 ms^{-1} with accuracy ±0.01 ms^{-1} for velocity and (20-80) % RH with accuracy ±1 % RH at 25°C]. The intensity of radiation from the sun was measured with a pyranometer [Model: Amprobe SOLAR-100, range 0-1999 Wm^{-2}] with reading accuracy ±1 Wm^{-2}. The initial and final content of moisture was determined by the oven method at 105 ° C.

3.3 Uncertainty

Uncertainty in measurements is caused by numerous factors such as calibration, environmental conditions, reading, and so on. Solar radiation, the temperature required for drying, the weight of GP and the velocity of air were some of the variables considered in the present experiments. Eq. (3.1) gives the uncertainty in the result (ΔZ_R), and the result R is the function of the independent variables$X_1, X_2, X_3 \ldots\ldots X_n$ [132] and is given in Table 3.1.

$$\Delta Z_R = \left[\left(\frac{\partial R}{\partial X_1} Z_1\right)^2 + \left(\frac{\partial R}{\partial X_2} Z_2\right)^2 + \left(\frac{\partial R}{\partial X_3} Z_3\right)^2 \ldots\ldots\ldots \left(\frac{\partial R}{\partial X_n} Z_n\right)^2\right]^{1/2} \quad (3.1)$$

where $Z_1, Z_2, Z_3 \ldots\ldots Z_n$ are the uncertainties in the independent variables. In case of velocity and temperature having gradients within the dryer system, the measurements are taken at multiple locations at each section of the dryer and the average values are reported.

Table 3.1 Values of uncertainties of the different parameters in the experiment

Parameter	Average Uncertainty
Moisture loss (weight)	± 0.01 (g)
Temperature	± 0.1 (°C)
Air velocity	± 0.01 (ms^{-1})
Solar radiation	± 1 (Wm^{-2})
Thermal efficiency in SAC	± 2.09 (%)
Thermal efficiency of the dryer	± 2.75 (%)

3.4 Performance Analysis

The first law of thermodynamics was used to carry out the energy analysis. In the analysis, the solar air collector and drying chamber were considered as steady flow devices.

According to the mass conservation principle in a system, the rate of incoming air is equal to the rate of outgoing air [133].

$$\sum \dot{m}_{i,a} = \sum \dot{m}_{o,a} \tag{3.2}$$

According to the energy conservation principle in a system, the rate of energy transfer into the system is equal to the rate of energy transfer out of the system.

$$\sum \dot{E}_{in,sys} = \sum \dot{E}_{out,sys} \tag{3.3}$$

$$\dot{H} + \sum \dot{m}_{i,a} \left(h_{i,a} + \frac{V^2{}_{i,a}}{2} + Z_{i,a} g \right) = \sum \dot{m}_{o,a} \left(h_{o,a} + \frac{V^2{}_{o,a}}{2} + Z_{o,a} g \right) + \dot{W} \tag{3.4}$$

In the present analysis, there isn't any work done by the dryer, and the difference between kinetic energy, and potential energy is neglected, as it is very small.

3.4.1 Energy analysis of SAC

Eqs. (3.5) and (3.6) were obtained from Eqs. (3.2) to (3.4) by applying the mass and energy conservation equation for a steady flow to SAC [133]. The air is assumed as an ideal gas.

$$\sum \dot{m}_{i,a} = \sum \dot{m}_{o,a} = \sum \dot{m}_a \tag{3.5}$$

$$\dot{H} = \dot{H}_{u,SAC} = \dot{H}_{in,SAC} - \dot{H}_{l,SAC} = \dot{m}_a \left(h_{out,a} - h_{in,a} \right) \tag{3.6}$$

The heat input of the SAC is given by

$$\dot{H}_{in,SAC} = \alpha \tau I A_{SAC} \tag{3.7}$$

The useful heat supplied by SAC is given [134]

$$\dot{H}_{u,SAC} = \dot{m}_a C_{pa} \left(T_{o,c} - T_{i,c} \right) \tag{3.8}$$

The energy efficiency of the corrugated collector is given by the ratio of useful heat supplied by SAC to heat input to SAC [135,136].

$$\eta_{e,SAC} = \frac{\dot{H}_{u,SAC}}{\dot{H}_{in,SAC}} = \frac{\dot{m}_a C_{pa} \left(T_{o,c} - T_{i,c} \right)}{\alpha \tau I A_{SAC}} \tag{3.9}$$

3.4.2 Energy analysis of the drying chamber

The energy input to the solar dryer is calculated as

$$E_{in,dry} = [(I_{SAC} \times A_{SAC}) + (I_d \times A_{md})] \times t_{dry} \quad (3.10)$$

For indirect solar drying, $(I_d \times A_{md}) = 0$. The energy input, $E_{in,dry}$ (kW-h) in the present analysis is identical to the solar thermal energy incident on the solar air heater integrated with dryer. SEC is the ratio of the energy input to the dryer to the amount of moisture evaporated [15].

$$SEC = \frac{E_{in,dry}}{m_w} \quad (3.11)$$

The ratio of the amount of energy required to remove moisture from product to the amount of energy input to the solar dryer is the solar dryer's total thermal efficiency [94].

$$\eta_{e,dry} = \frac{m_w Q_L}{E_{in,dry}} \quad (3.12)$$

3.5 Drying Kinetics

For the trials and OSD, the drying kinetics of product were investigated. To check the drying kinetics, the samples in each experiment were weighed at a 1 h interval until the weight did not show any change. Eleven different drying models available in the literature were tested to find the best fit for each batch and OSD of experiments. Table 3.2 gives the list of the eleven drying models considered for the analysis of the drying kinetics. Eqs.(3.13)-(3.15) can be used to calculate the MC and moisture ratio (MR) of product during the drying experiments [132].

$$MC_{GP} = \frac{m_{i,GP} - m_{j,GP}}{m_{i,GP}} \quad (3.13)$$

$$MR_{GP} = \frac{M_{GP,t} - M_{GP,e}}{M_{GP,i} - M_{GP,e}} \quad (3.14)$$

The simplified MR:

$$MR = \frac{M_{GP,t}}{M_{GP,i}} \quad (3.15)$$

The values of $M_{GP,e}$ are comparatively smaller than $M_{GP,t}$ and $M_{GP,i}$, and subsequently ignored. In the case of uniform relative humidity of the drying air, Eq. (3.14) is used. The variation in relative humidity, on the other hand, leads to Eq. (3.15). The variation of MR with time was plotted. The non-linear regression analysis was carried out in Matlab. The values of root mean square error ($RMSE$), reduced chi-square (χ^2), and coefficient of

determination (R^2) were calculated using Eq. (3.16), Eq. (3.17), and Eq. (3.18), respectively. The lower values of *RMSE*, and χ^2 along with higher values of R^2 were considered for the determination of the best drying model [14].

$$RMSE^2 = \frac{1}{n}\sum_{i=1}^{n}(MR_{pr,i} - MR_{ex,i})^2 \tag{3.16}$$

$$\chi^2 = \frac{\sum_{i=1}^{n}(MR_{ex,i} - MR_{pr,i})^2}{n - z} \tag{3.17}$$

$$R^2 = 1 - \frac{\sum_{i=1}^{n}(MR_{pr,i} - MR_{ex,i})^2}{\sum_{i=1}^{n}(MR_{avp} - MR_{ex,i})^2} \tag{3.18}$$

Table 3.2 Different mathematical models to characterize the drying kinetics of *Garcinia pedunculata*.

Model No.	Name of the Model	Model equation	References
A.	Newton	$MR = exp(-kt)$	[137]
B.	Page	$MR = exp(-kt^n)$	[93]
C.	Modified Page	$MR = exp(-kt)^n$	[138]
D.	Henderson and Pabis	$MR = a\,exp(-kt)$	[26]
E.	Modified Henderson and Pabis	$MR = a\,exp(-kt) + b\,exp(-gt) + c\,exp(-ht)$	[101]
F.	Logarithmic	$MR = a\,exp(-kt) + c$	[116]
G.	Two Term	$MR = a\,exp(-k_1t) + b\,exp(-k_2t)$	[139]
H.	Two Term exponential	$MR = a\,exp(-kt) + (1-a)\,exp(kat)$	[12]
I.	Wang and Singh	$MR = 1 + at + bt^2$	[17]
J.	Diffusion approximation model	$MR = a\,exp(-kt) + (1-a)\,exp(kbt)$	[85]
K.	Midilli and Kucuk	$MR = a\,exp(-kt^n) + bt$	[140]

3.6 Economic Analysis

The economic study determines the price-effectiveness of the solar dryer for commercial use with various agricultural products. In this study, life cycle savings (LCS) and payback period methods were employed to study the viability of the solar dryer for drying product [109]. The price of fresh product per kg of dried product (C_{dGP}) is determined by Eq. (3.18).

$$C_{dGP} = C_{fGP} \times \frac{m_{fGP}}{m_{dGP}} \tag{3.18}$$

where, C_{fGP} (INR/kg), m_{fGP} (kg) is the price and mass of fresh product, respectively and m_{dGP} is the mass of dried product (kg) per batch.

The price needed to dry 1 kg of product (C_{ds}) is determined by using Eq. (3.19).

$$C_{ds} = C_{dGP} + C_{sGP} \tag{3.19}$$

where C_{sGP} is the price of drying per kg of dried product.

The annualized price (C_{anc}) of the solar dryer for drying the product is given by

$$C_{anc} = C_{acc} + C_{amc} + C_{rfc} + C_{ec} - S_v \tag{3.20}$$

where C_{acc} is the annual capital price, C_{amc} is the annualized maintenance price and C_{rfc} is the annual running fuel price. For the solar dryer, the annual running fuel price is zero. C_{ec} is the electricity price, which is again zero as the dc motor runs on a solar panel. S_{av} is the annualized salvage value. C_{amc} is a fixed percentage of C_{acc} (assumed 10 % of C_{acc}).

The annualized capital price C_{acc} is given by

$$C_{acc} = C_{cc} \times R_f \tag{3.21}$$

where C_{cc} is the capital price of the dryer and R_f is capital recovery factor respectively. The capital recovery factor R_f is given by

$$R_f = \frac{d \times (1+d)^k}{(1+d)^k - 1} \tag{3.22}$$

where d is the rate of interest (in %) on the investment and k is the life of the domestic solar dryer.

Salvage fund factor (S_F) is given as

$$S_F = \frac{d}{(1+d)^k - 1} \tag{3.23}$$

Annualized salvage value is given as

$$S_a = S \times S_F \tag{3.24}$$

where S is the salvage value of 10 % of the capital price.

Mass of product dried per year in the solar dryer m_{yGP}

$$m_{yGP} = m_{dGP} \times \frac{t_s}{t_d} \tag{3.25}$$

The price of solar drying $(\mathrm{C_{sGP}})$ for 1 kg of dried product in the dryer is given by

$$C_{sGP} = \frac{C_{anc}}{m_{yGP}} \tag{3.26}$$

Savings for product per kg (S_{kg}) is the difference between the expense of the product available in the market (C_{mGP}) and the expense needed to dry 1 kg of product in the dryer (C_{ds}) evaluated using Eq. (3.27)

$$S_{kg} = C_{mGP} - C_{ds} \tag{3.27}$$

Saving per day (S_d) is calculated by

$$S_d = \frac{S_b}{t_d} = \frac{S_{kg} \times m_{dGP}}{t_d} \tag{3.28}$$

where S_b is the savings and t_d (in days) is the drying time required in each batch. Yearly savings of drying of product (S_k) in the (j^{th}) year is calculated using the following equation

$$S_k = S_d \times t_{sun} \times (1+i)^{j-1} \tag{3.29}$$

where i is the inflation rate

Payback period (P_p) of the developed solar dryer is given [132]

$$P_p = \frac{ln\left[1 - \frac{C_{cc}}{S_1}(d-i)\right]}{ln\left[\frac{1+i}{1+d}\right]} \tag{3.30}$$

where S_1 is saving for the first year.

The rate of interest and inflation were taken as 10 % [132] and 4.62 %, respectively. The maintenance price and salvage value were taken as 10 % of the annualized capital price and 10 % of the capital price of the dryer, respectively [132]. The life of the dryer has been assumed as 10 years.

3.7 Results and Discussion

3.7.1 Performance analysis of *Garcinia pedunculata*

The experiments for drying of *Garcinia pedunculata* were carried out from 12th to 14th October (first batch) and 16th to 18th October (second batch) in Tezpur University campus (latitude 26°42' 03″N and longitude 92°49'49″E), Assam in India. It was found that the temperature of ambient air varied from 29.5 °C to 33.8 °C for the first batch and 29.2 °C to 34.3 °C for the second batch. Average solar radiation was 920 Wm^{-2} for the first batch and 928 Wm^{-2} for the second batch as described in Figure 3.3 and Figure 3.4 respectively. During the drying period of the first batch, the intensity of radiation from the sun was recorded highest at 11:30 h for the first (1063 Wm^{-2}) and second (1043 Wm^{-2}) day. However, the intensity of solar radiation was recorded highest at 12:30 h (993 Wm^{-2}) for the third day. For the second batch, on the first day, the intensity of radiation from the sun was recorded highest at 11:30 h but it dropped subsequently at the latter part of the day. The highest radiation was recorded at 11:30 h for the first (1055 Wm^{-2}), second (1084 Wm^{-2}) and third day (1005 Wm^{-2}). In between 10:30 h and 11:30 h, the maximum radiation was recorded for all three days for the second batch. An anemometer was used to measure the average velocity of air close to the drying trays. The air velocity was 0.1 ms^{-1} and the rate of mass flow was found to be 0.00735 kgs^{-1}.

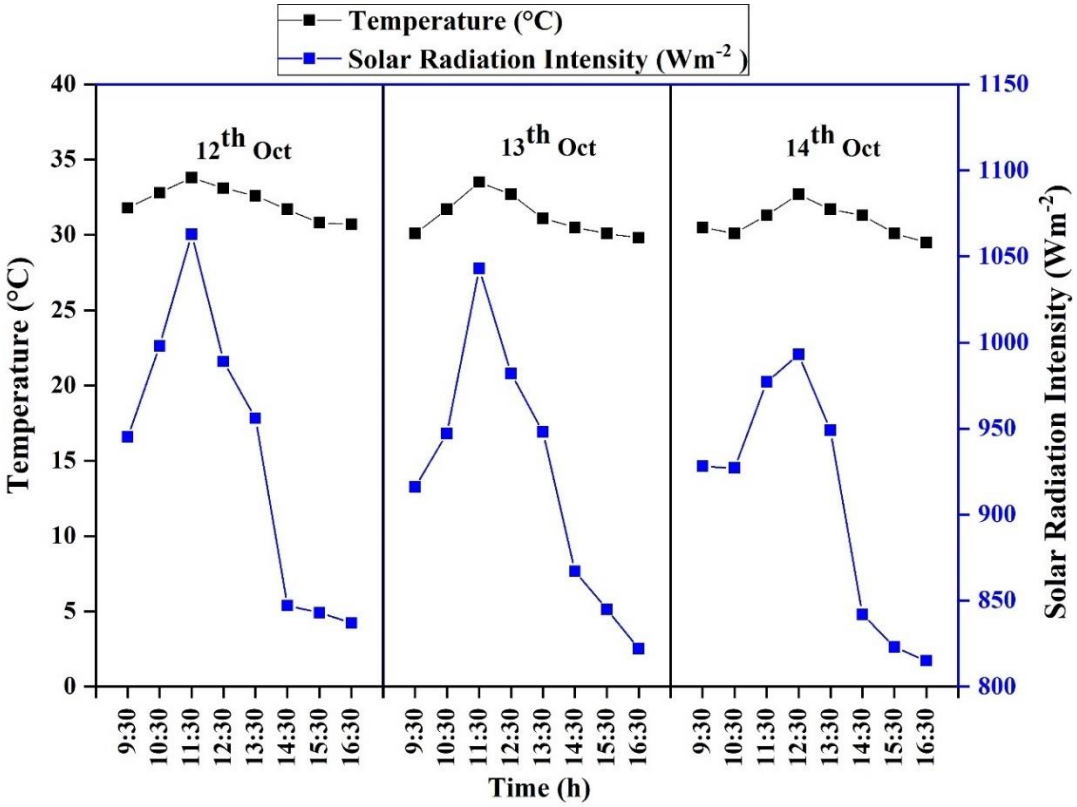

Figure 3.3 The intensity of solar radiation and the temperature of the ambient variation with the drying time for the first batch.

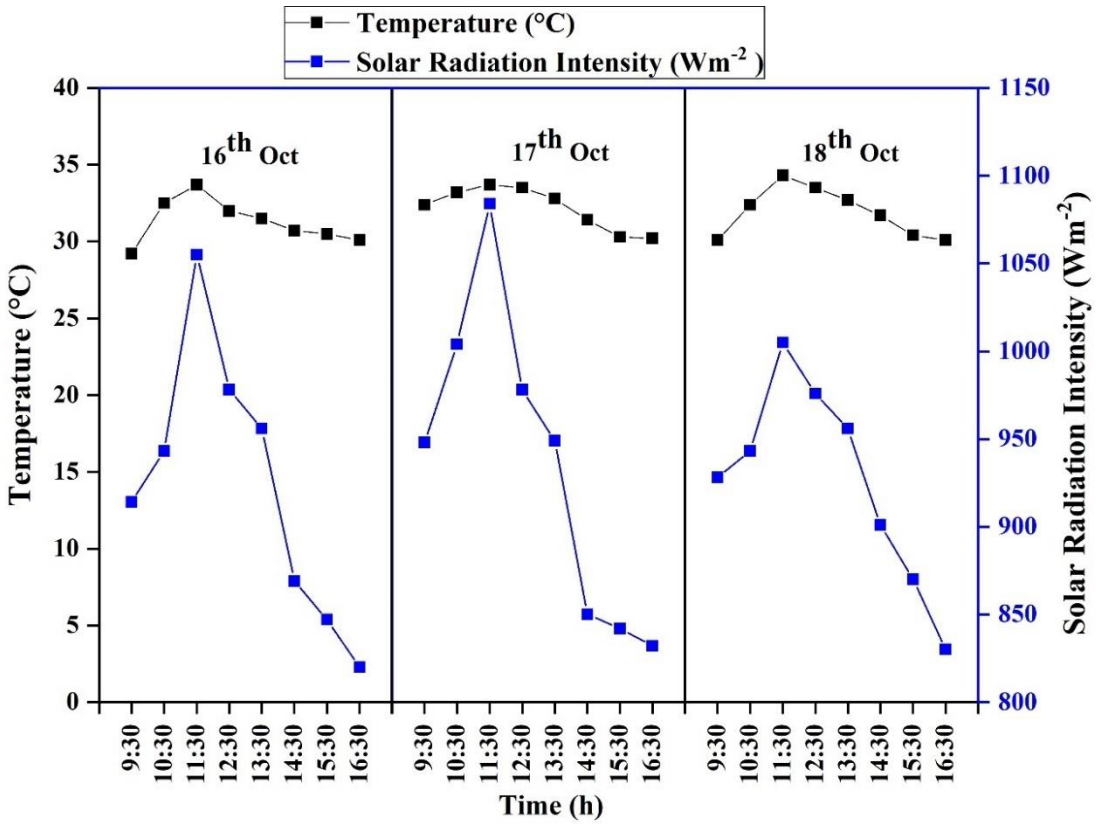

Figure 3.4 The intensity of solar radiation and the temperature of the ambient variation with the drying time for the second batch.

The first batch of samples dried on FCCSD exhibited inlet temperatures ranging from 31.9 °C to 35.5 °C and outlet temperatures ranging from 61.9 °C to 84.3 °C, as illustrated in Figure 3.5. Similarly, for the second batch, the inlet temperatures ranged from 30.5 °C to 35.9 °C and the outlet temperatures ranged from 61.1 °C to 84.5 °C, as depicted in Figure 3.6. The corrugated absorber plate temperature of the solar air heater with FCCSD was found to be 83.1 °C to 114.3 °C for the first batch and 83.4 °C to 115.4 °C for the second batch. The air temperatures varied at different positions of FCCSD as plotted. The absorber plate was found to attain its highest temperature at around 11:30 h for both the batches. The temperatures and humidity of FCCSD were recorded till 12:30 h of the second day. However, the ambient temperature and ambient humidity were recorded until 16:30 h of the third day since the OSD of GP continued for both the batches.

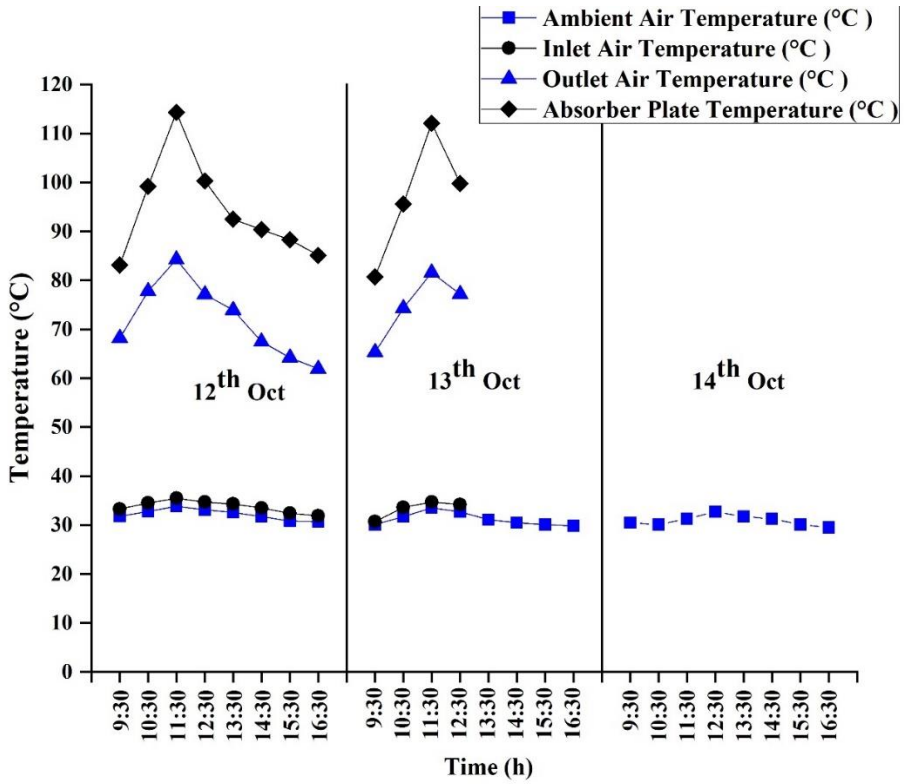

Figure 3.5 The ambient, inlet, outlet and absorber plate temperature variation with the drying time for the first batch

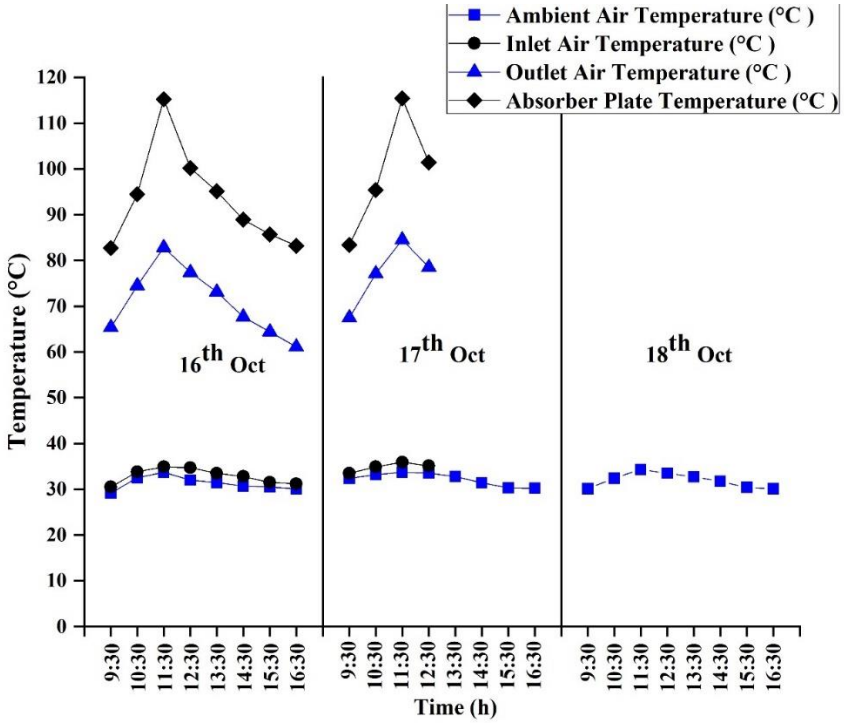

Figure 3.6 The ambient, inlet, outlet and absorber plate temperature variation with the drying time for the second batch.

The relative humidity of air at the inlet, outlet and ambient were presented in Figure 3.7 and Figure 3.8. The ranges of relative humidity at the inlet, outlet and ambient were found to be 45.6 % to 65.5 %, 45.8 % to 86.7 % and 61.7 % to 82.3 % respectively for the first batch and 45.7 % to 65.1 %, 45.6 % to 86.6 % and 64.7 % to 80.6 % respectively for the second batch. The first batch analysis showed the relative to be lowest around 11:30 h for the inlet and ambient for the first day and second day. The third day recorded the lowest ambient humidity at 12:30 h. The analysis of the second batch indicated that the lowest relative humidity occurred at approximately 11:30 a.m. for both the inlet and ambient conditions on the first day. The humidity records lowest at the outlet on the second day at around 12:30 h because of the evaporation of the moisture from the sample due to free convection. However, on the third day, the ambient humidity showed variation because of somewhat cloudiness.

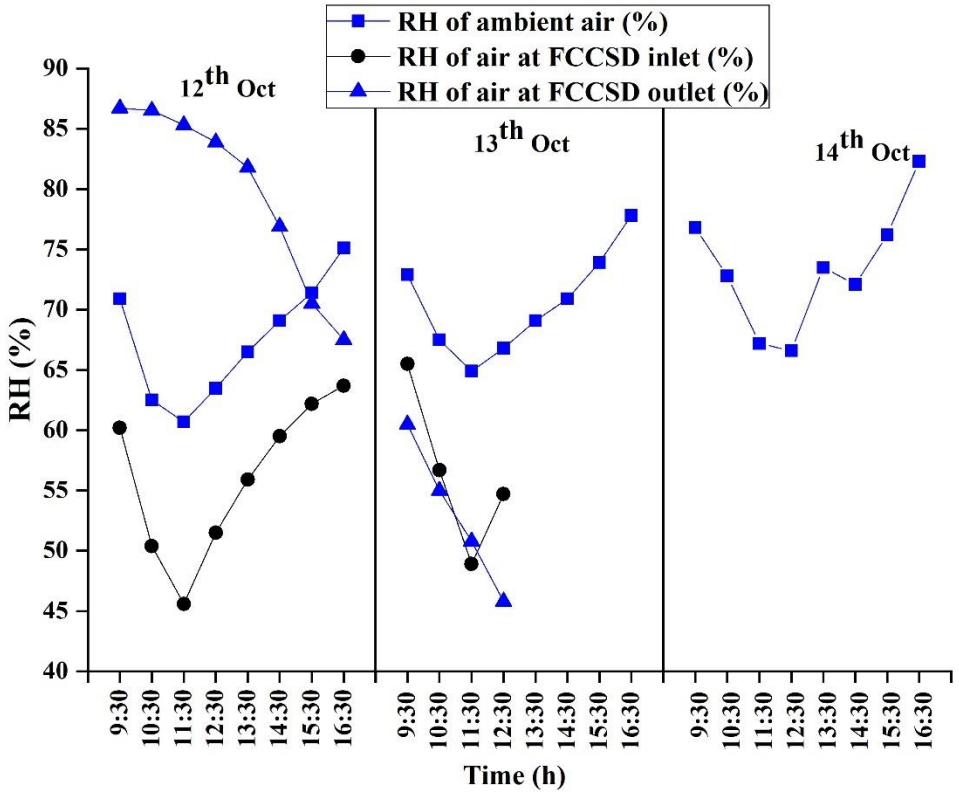

Figure 3.7 The relative humidity of air at the inlet, outlet and ambient variation with the drying time for the first batch

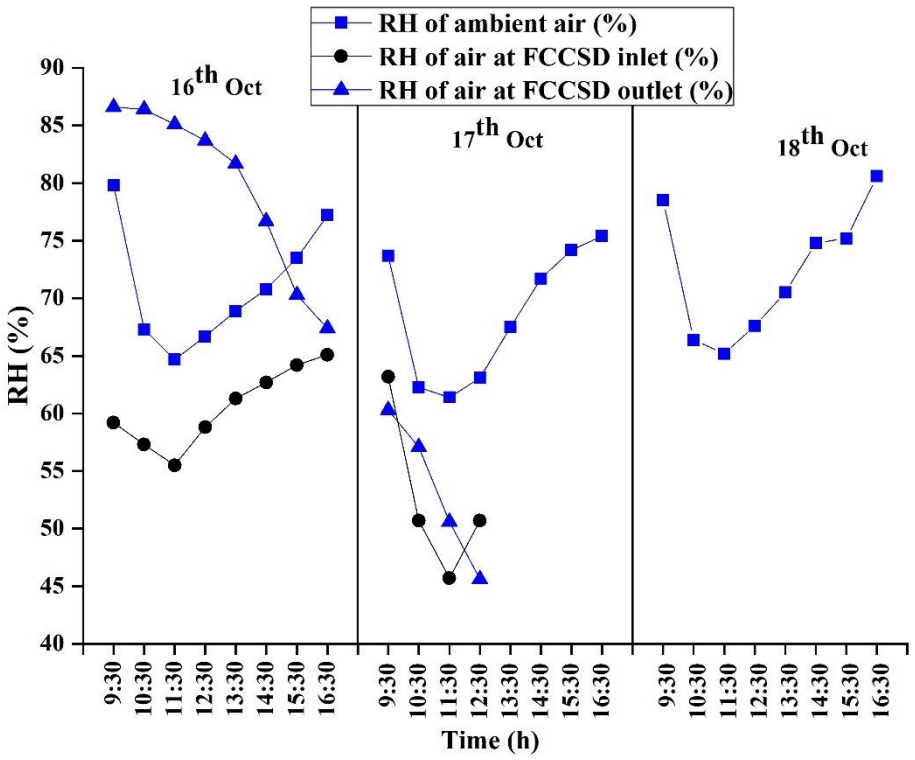

Figure 3.8 The relative humidity of air at the inlet, outlet and ambient variation with the drying time for the second batch.

The useful heat gain with the time required for drying was calculated from Eq. (3.8). From the equation, the maximum heat gain was found to be 360.47 W for the first day and 346.43 W for the second day for the first batch as shown in Figure 3.9. The maximum heat gain was found to be 353.83 W for the first day and 358.99 W for the second day for the second batch as shown in Figure 3.10. The average useful heat gain for the first and the second batch was found to be 289.31 W and 290.36 W respectively. On all the days, the maximum useful heat gain was found at 11:30 h. At the latter part of the day the useful heat gain lowered.

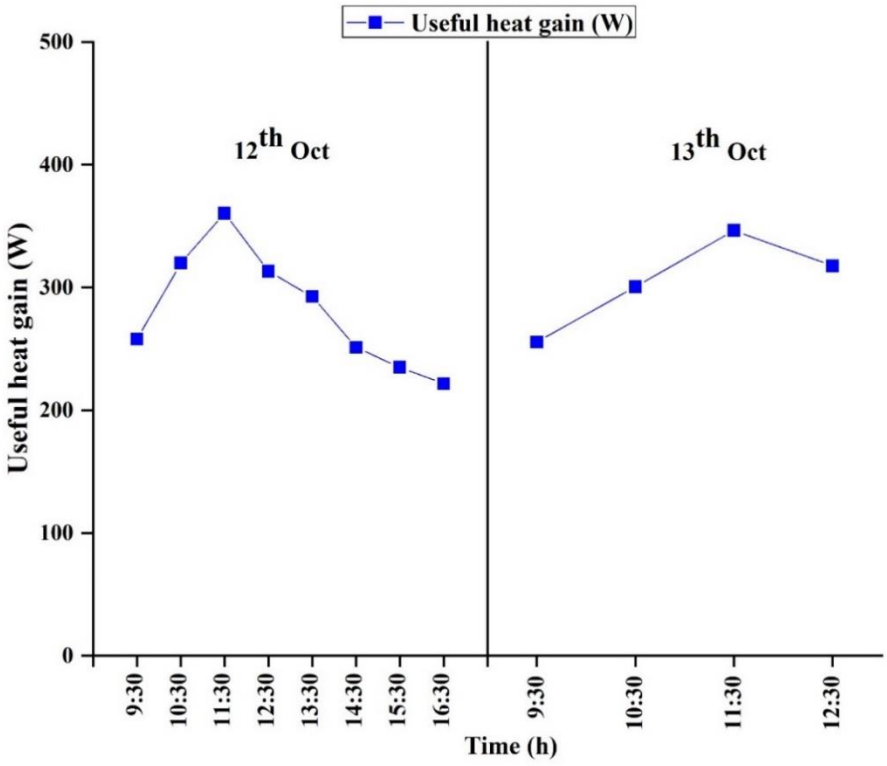

Figure 3.9 Useful heat gain variation with the drying time for the first batch.

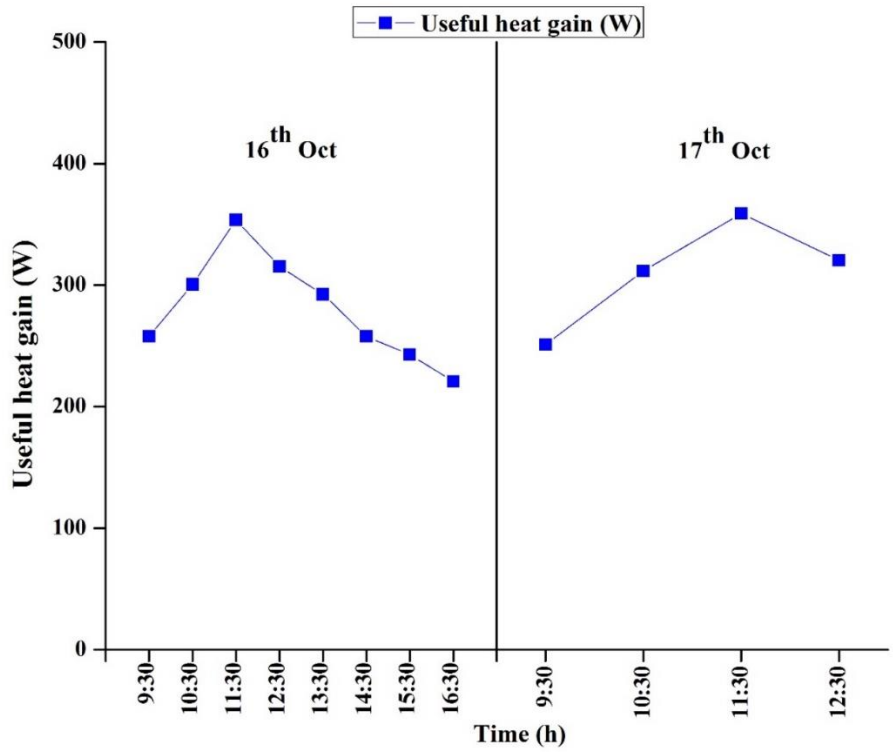

Figure 3.10 Useful heat gain variation with the drying time for the second batch.

The absorber plate of the solar air heater was corrugated that helped to enhance heat transfer with local turbulence by breaking the laminar sub-layer. The thermal efficiency variation of integrated solar air heater with drying time was calculated from Eq. (3.9) exhibited in Figure 3.11 and Figure 3.12 for the first and second batch respectively. Considering the first batch, the range of thermal efficiency was found to be 29.00 % to 37.14 % with an average of 33.29 %. The maximum was found at 11:30 h for both the days. The second batch exhibits the variation from 29.02 % to 36.73 % with the maximum at 11:30 h. The efficiency of the air heater on the following day was calculated to 12:30 h for both the batches.

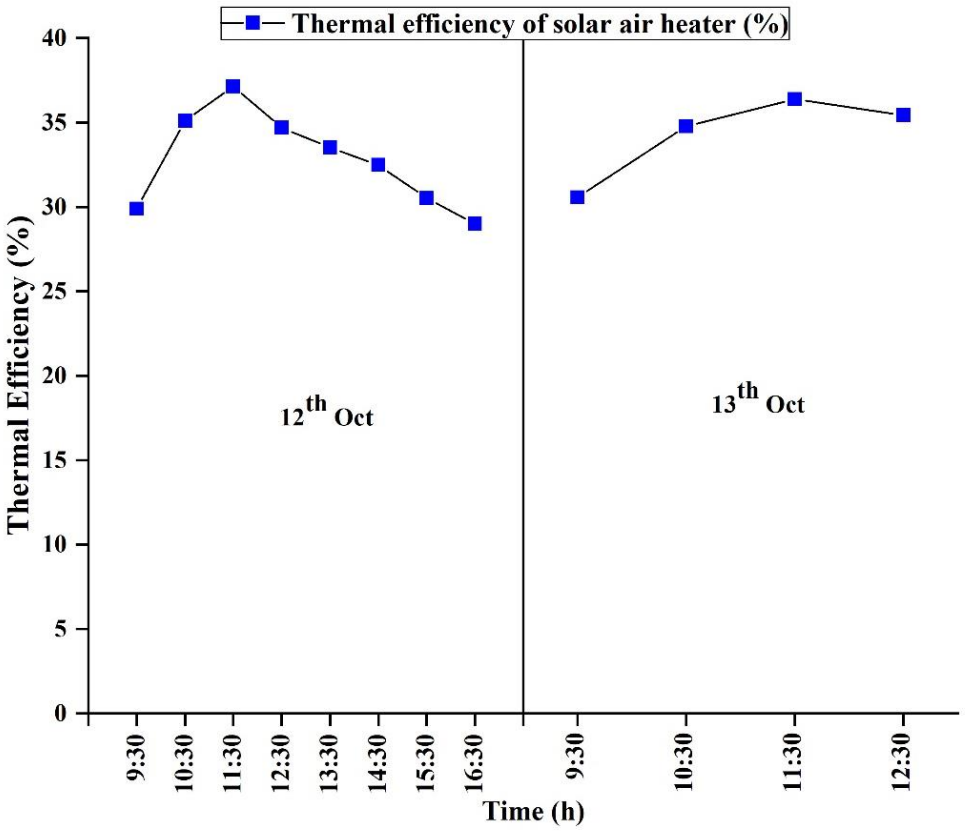

Figure 3.11 Thermal efficiency variation with the drying time for the first batch.

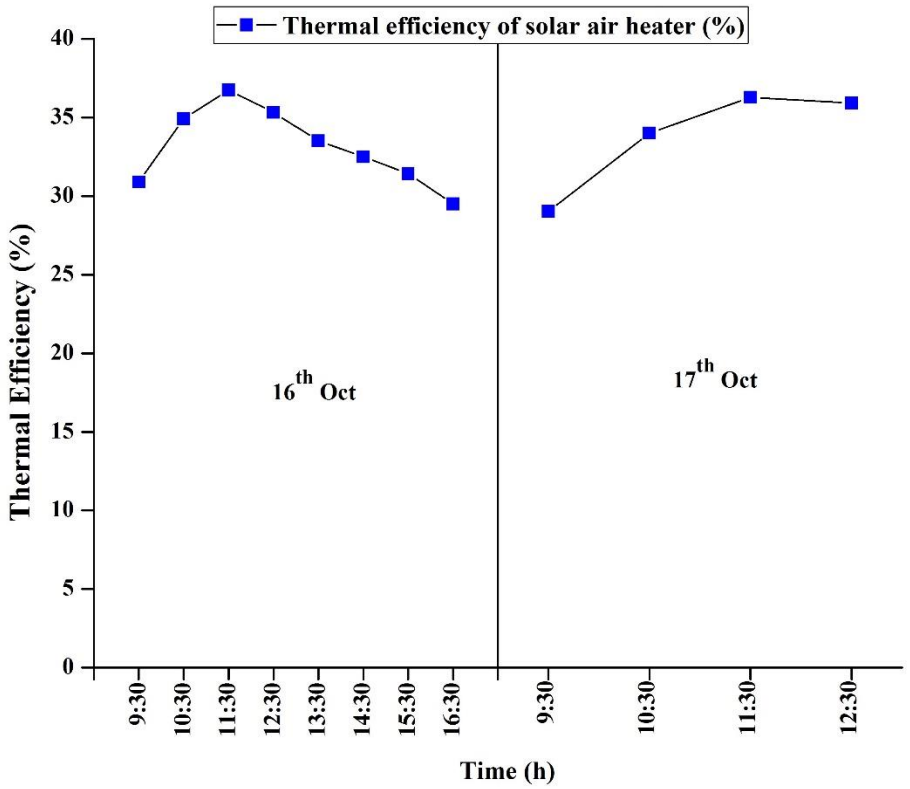

Figure 3.12 Thermal efficiency variation with the drying time for the second batch.

The specific energy consumption and efficiency of the dryer were calculated using Eq. (3.11) and Eq. (3.12) respectively and plotted in Figure 3.13 and Figure 3.14 for the first and second batch respectively. Three air temperature readings were repeated to estimate the average temperature. The average specific energy consumption and average efficiency of the dryer for the first batch were found to be 68.00 $kWhkg^{-1}$ and 10.69 % respectively. The average specific energy consumption and average efficiency of the dryer for the second batch were found to be 65.54 $kWhkg^{-1}$ and 10.77 % respectively. Higher specific energy consumption would indicate a less efficient use of solar energy. This indicates that the dryer capacity was not fully utilized. Moreover, beyond 8 h of the drying period, the moisture removal rate was drastically reduced. These are the reasons for its low overall efficiency. Another two perforated trays may easily fit into the FCCSD and the drying air may be utilized more effectively.

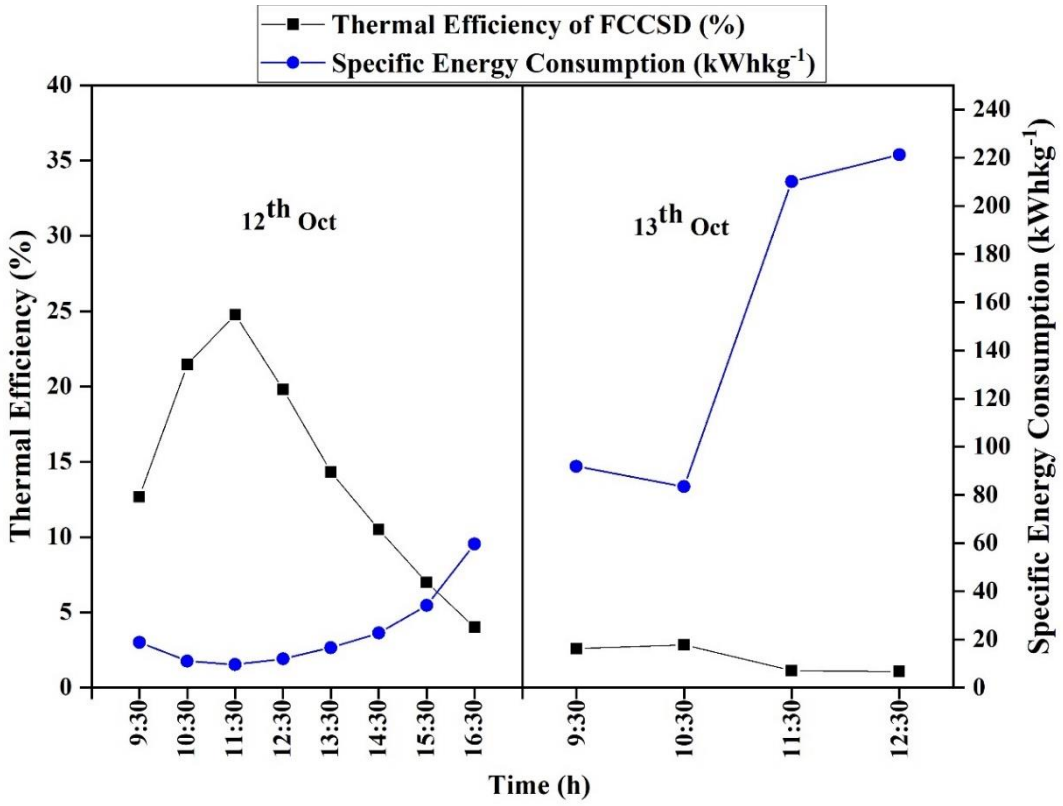

Figure 3.13 The thermal efficiency and specific energy consumption variation with the drying time for the first batch.

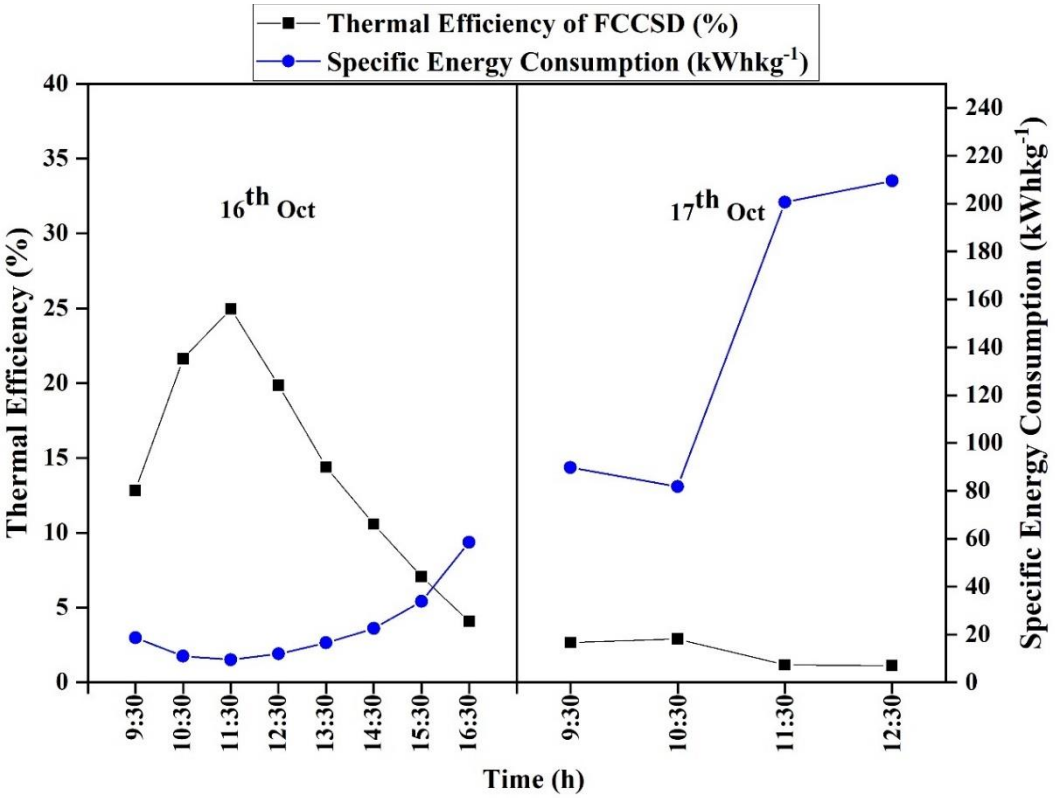

Figure 3.14 The thermal efficiency and specific energy consumption variation with the drying time for the second batch.

3.7.2 Drying kinetics of GP

From the initial MC of 88 % (w.b.), the final MC was decreased to 7.22 % (w.b.) for the first batch and 7.1 % (w.b.) for the second batch in 28 h in FCCSD as shown in Figure 3.15 and Figure 3.16. But the product dried near the outlet took lesser time because of the higher temperature at the outlet. Thereby the locations of perforated trays were rotated 180° to maintain uniform drying. The OSD of GP took 55 h to reach to a final MC of 10.18 % (w.b.) and 10.08 % (w.b.) for the first and second batch respectively.

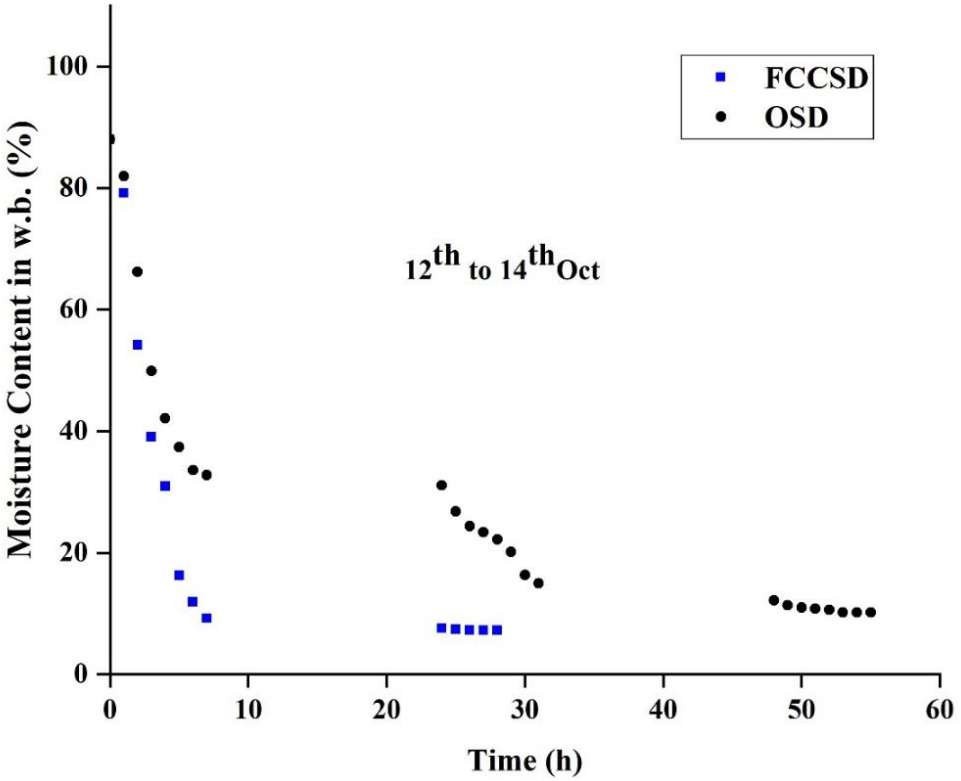

Figure 3.15 MC variation of GP with drying time for the first batch.

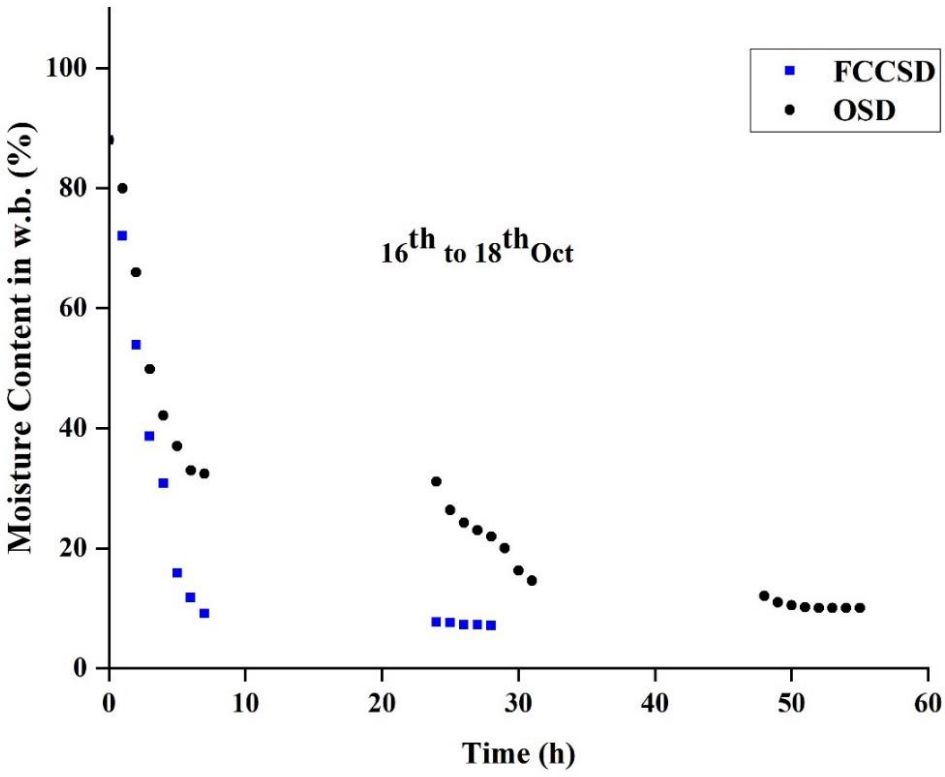

Figure 3.16 MC variation of GP with drying time for the second batch.

The variation in drying rate with the time required for drying is described in Figure 3.17 and Figure 3.18 for the first and second batch respectively. The drying rate of GP in FCCSD was observed to be faster than in OSD. The drying rate was found to be at the peak during the initial h of the day of drying for both the batches. When the temperature was highest which is around 10:30 h and 11.30 h, the drying rate was found to be maximum for both the cases. After 24 h the drying rate of FCCSD was dropped eventually when compared with OSD because of the low MC of GP.

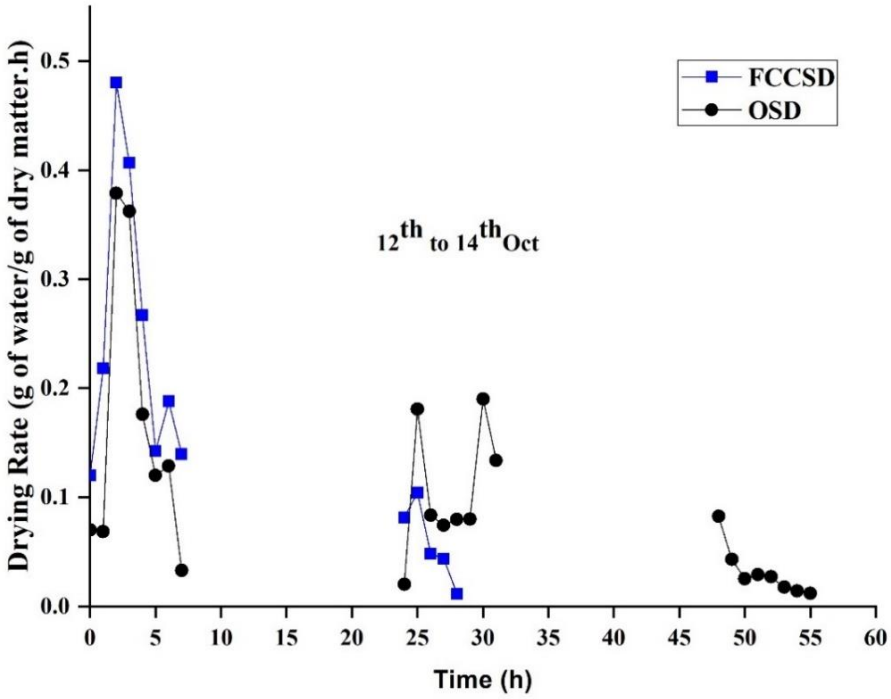

Figure 3.17 Drying rate variation with drying time for the first batch.

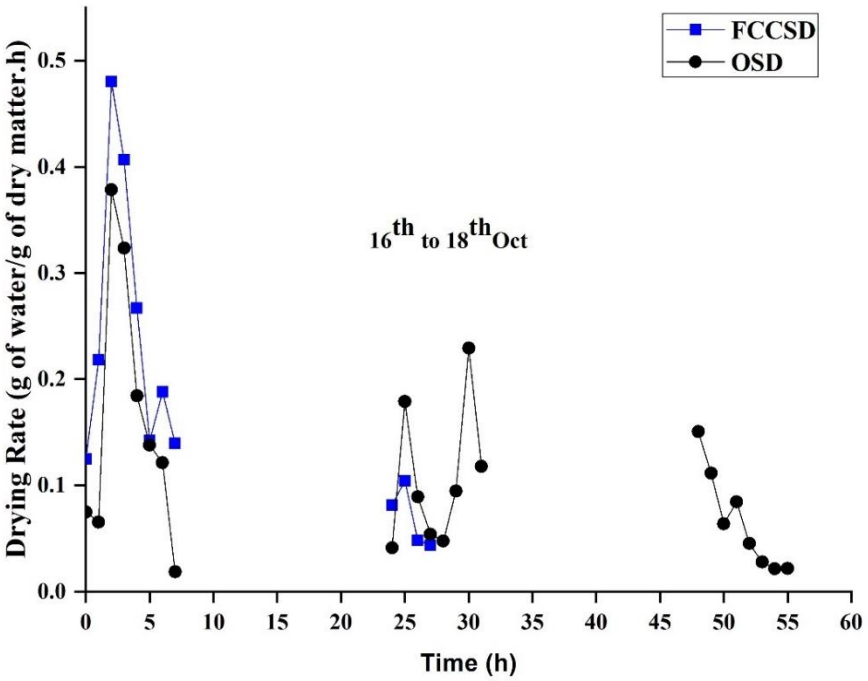

Figure 3.18 Drying rate variation with drying time for the second batch.

The MR of GP with drying time is plotted in Figure 3.19 and Figure 3.20 for the first and second batch respectively. To locate the best drying model, the MR versus drying time is required to carry out the non-linear regression analysis. Table 3.3 and Table 3.4 give the regression analysis of FCCSD and OSD respectively for the first batch and Table 3.5 and Table 3.6 give the regression analysis of FCCSD and OSD respectively for the second batch. The selection of the most suitable drying model was done by fitting the moisture ratio data from the experiment and open sun drying to the drying models mentioned in Table 3.2. Based on the higher values of R^2 and lower values of χ^2 and RMSE, the best model was selected and from the analysis, it was found that Midilli and Kucuk for FCCSD and Two Term model for OSD gave higher value of R^2 and lower values of χ^2 and RMSE for both the batches. For the first batch, the values of $R^2 = 0.9973$, $\chi^2 = 0.0003$ and $RMSE = 0.01882$ was found for FCCSD. The values of $R^2 = 0.9842$, $\chi^2 = 0.0012$ and $RMSE = 0.03437$ for OSD. Again, for the second batch, the values of $R^2 = 0.9969$, $\chi^2 = 0.0004$ and $RMSE = 0.02016$ was found for FCCSD. The values of $R^2 = 0.9839$, $\chi^2 = 0.0012$ and $RMSE = 0.0348$ for OSD. Commonly, it is anticipated that an increase in the number of free parameters would result in superior fitting. Nevertheless, this presumption may not always hold true. In this instance, it was observed that a model featuring merely four free

parameters exhibited superior performance compared to a counterpart with six free parameters across both experimental batches.

The Midilli and Kucuk model for FCCSD for the first batch is expressed as

$$MR = 1.004 \exp(-0.2314t^{1.257}) + 0.002966t \quad (3.31)$$

And the Two Term model for OSD for the first batch is expressed as

$$MR = 0.5143 \exp(-0.08116\ t) + 0.5364 \exp(-0.409\ t) \quad (3.32)$$

The Midilli and Kucuk model for FCCSD for the second batch is expressed as

$$MR = 1.005\ exp(-0.2274t^{1.269}) + 0.002943t \quad (3.33)$$

29)

And the Two Term model for OSD for the second batch is expressed as

$$MR = 0.5143\ \ exp(-0.08116\ t) + 0.5364\ \ exp(-0.409\ t) \quad (3.34)$$

The comparison of experimental and predicted MR for FCCSD of GP by the Midilli and Kucuk is given in Figure 3.21 and Figure 3.22 for the first and second batch respectively. Similarly, the comparison of experimental and predicted MR for OSD of GP by Two Term model is given by Figure 3.23 and Figure 3.24 From these figures, it can be concluded that the straight line for FCCSD and OSD validate the suitability for the models.

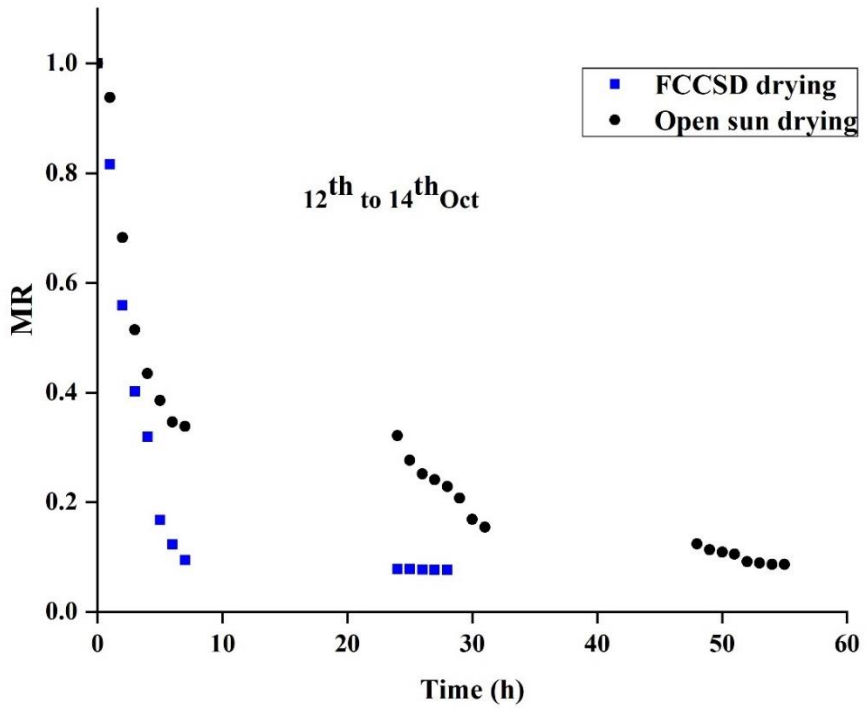

Figure 3.19 Moisture ratio variation of GP with drying time for the first batch.

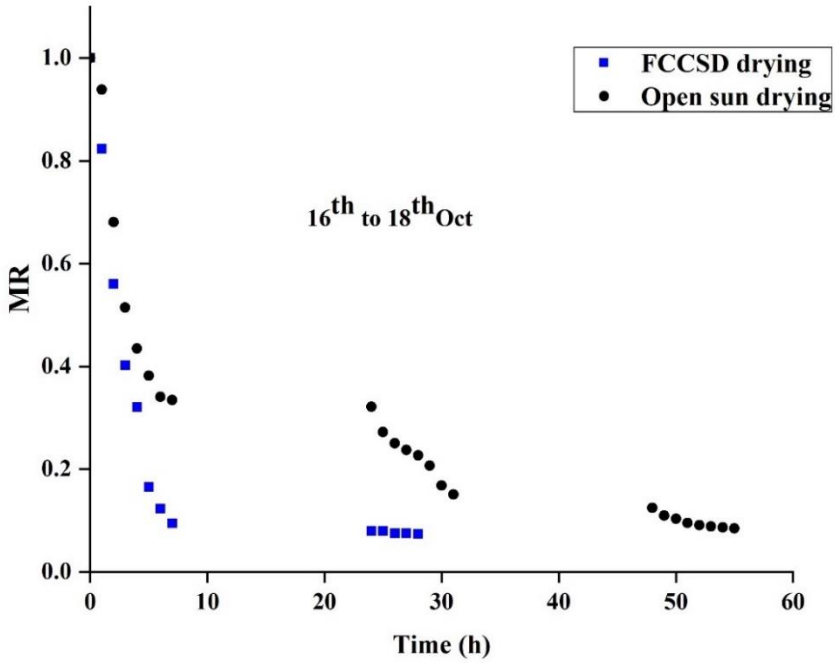

Figure 3.20 Moisture ratio variation of GP with drying time for the second batch.

Table 3.3 Fitting statistics of thin layer drying model of FCCSD of GP for the first batch.

Model No.	Coefficients and constants	R^2	χ^2	$RMSE$
A.	$k = 0.305$	0.9648	0.0034	0.05867
B.	$k = 0.2308; n = 1.224$	0.9717	0.0030	0.05491
C.	$k = 0.8801; n = 0.3465$	0.9648	0.0037	0.06128
D.	$k = 1.04; a = 0.3178$	0.9667	0.0035	0.0596
E.	$a = -0.1346;\ b = 2.14;\ c = 1.005; g = 0.4115;$ $h = 0.506;\ k = 7.46$	0.9723	0.0046	0.06818
F.	$a = 0.9865; k = 0.3646; c = 0.06268$	0.9855	0.0017	0.04127
G.	$a = -0.003263;\ k_1 = -0.119; b = 1.039;$ $k_2 = 0.3228$	0.9907	0.0012	0.0348
H.	$a = 1.001; k = 0.0.305$	0.9648	0.0037	0.06128
I.	$a = -0.1739; b = 0.005285$	0.8722	0.0136	0.116
J.	$a = 2.077;\ b = 0.8602;\ k = 0.2599$	0.9653	0.0040	0.06381
K.	$\boldsymbol{a = 1.004; b = 0.002966;\ k = 0.2314;}$ $\boldsymbol{n = 1.257}$	**0.997**	**0.0003**	**0.0188**

Table 3.4 Fitting statistics of thin layer drying model of OSD of GP for the first batch.

Model No.	Coefficients and constants	R^2	χ^2	$RMSE$
A.	$k = 0.1478$	0.9458	0.0034	0.05935
B.	$k = 0.2394; n = 0.769$	0.9745	0.0030	0.04167
C.	$k = 0.6477; n = 0.2282$	0.9458	0.0037	0.06069
D.	$k = 0.9337; a = 0.1365$	0.9519	0.0035	0.05718
E.	$a = 0.282;\ b = 0.5174;\ c = 0.25;$ $g = 0.08036;\ h = 0.4105;\ k = 0.4116$	0.9842	0.0046	0.03623
F.	$a = 0.9061; k = 0.2055; c = 0.1023$	0.9754	0.0017	0.04188
G.	$\boldsymbol{a = 0.5171; k_1 = 0.080; b = 0.5331;}$ $\boldsymbol{k_2 = 0.4108}$	**0.9842**	**0.0012**	**0.03437**
H.	$a = 0.2588; k = 0.4394$	0.9738	0.0037	0.04222
I.	$a = -0.109; b = 0.00319$	0.8883	0.0136	0.08713
J.	$a = 0.5041;\ b = 0.2189;\ k = 0.3587$	0.9821	0.0040	0.03571
K.	$a = 1.038; b = 0.00194; k = 0.2462;$ $n = 0.8066$	0.9776	0.0003	0.04097

Table 3.5 Fitting statistics of thin layer drying model of FCCSD of GP for the second batch.

Model No.	Coefficients and constants	R^2	χ^2	$RMSE$
A.	$k = 0.3041$	0.9642	0.0035	0.0594
B.	$k = 0.2261; n = 1.238$	0.972	0.0030	0.05493
C.	$k = 0.7371; n = 0.4126$	0.9642	0.0038	0.06204
D.	$k = 0.3178; a = 1.043$	0.9664	0.0036	0.06015
E.	$a = 0.253;\ b = 10.32;$ $c = 9.518; g = 0.2173; h = 0.2135;\ k = 0.666$	0.9616	0.0064	0.08055
F.	$a = 0.9898; k = 0.3636; c = 0.0618$	0.9845	0.0018	0.0428
G.	$a = -3.629; k_1 = 0.2341; b = 4.668;$ $k_2 = 0.2504$	0.9668	0.0043	0.0661
H.	$a = 1.807; k = 0.4359$	0.972	0.0030	0.0549

I.	$a = -0.173; b = 0.005276$	0.8715	0.0138	0.1176
J.	$a = 3.871;\ b = 0.9326;\ k = 0.2496$	0.9648	0.0041	0.06453
K.	$\boldsymbol{a = 1.005; b = 0.002943;\ k = 0.2274;}$ $\boldsymbol{n = 1.269}$	**0.9969**	**0.0004**	**0.02016**

Table 3.6 Fitting statistics of thin layer drying model of OSD of GP for the second batch.

Model No.	Coefficients and constants	R^2	χ^2	$RMSE$
A.	$k = 0.1493$	0.9468	0.0034	0.059
B.	$k = 0.2395; n = 0.7726$	0.9742	0.0017	0.04202
C.	$k = 0.3934; n = 0.3794$	0.9468	0.0036	0.06033
D.	$k = 0.1383; a = 0.936$	0.9524	0.0032	0.05708
E.	$a = 1.177;\ b = 6.556;\ c = -6.331;$ $g = 0.0056;\ \ h = .0050; k = 0.4874$	0.8451	0.0129	0.1138
F.	$a = 0.9093; k = 0.2064; c = 0.1001$	0.9753	0.0017	0.04211
G.	$\boldsymbol{a = 0.5143; k_1 = 0.08116; b = 0.5364;}$ $\boldsymbol{k_2 = 0.409}$	**0.9839**	**0.0012**	**0.0348**
H.	$a = 0.2611; k = 0.4392$	0.9739	0.0017	0.04226
I.	$a = -0.1095; b = 0.00321$	0.8882	0.0076	0.08745
J.	$a = 0.5055;\ b = 0.222;\ k = 0.3581$	0.9818	0.0013	0.03615
K.	$a = 1.037; b = 0.00525; k = 0.2357;$ $n = 0.8777$	0.9729	0.0022	0.04721

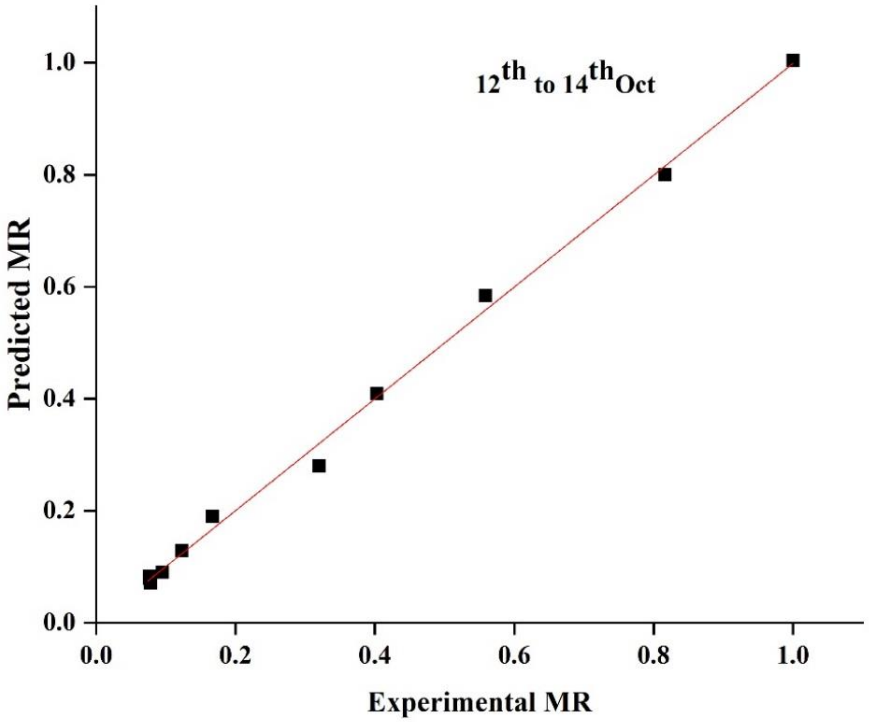

Figure 3.21 Comparison of predicted and experimental MR for FCCSD of GP by Midilli and Kucuk model for the first batch.

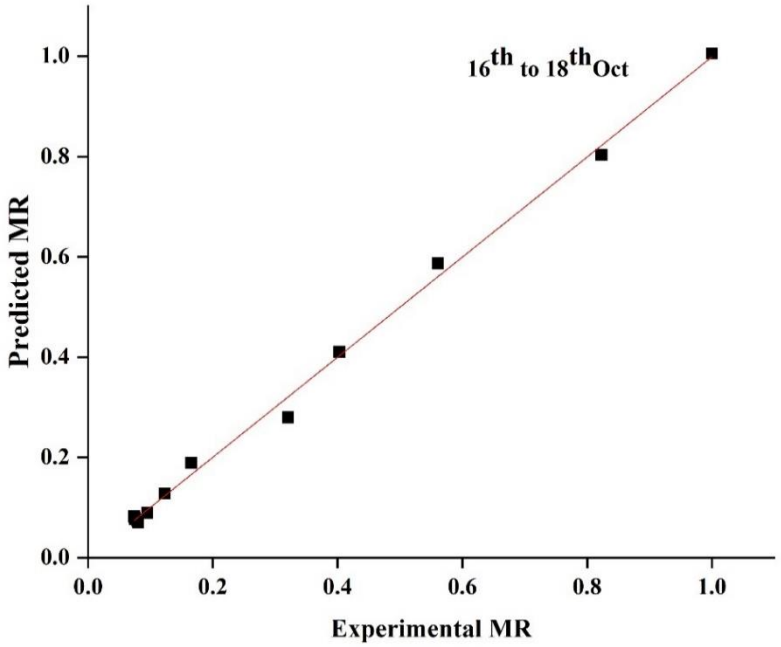

Figure 3.22 Comparison of predicted and experimental MR for FCCSD of GP by Midilli and Kucuk model for the second batch.

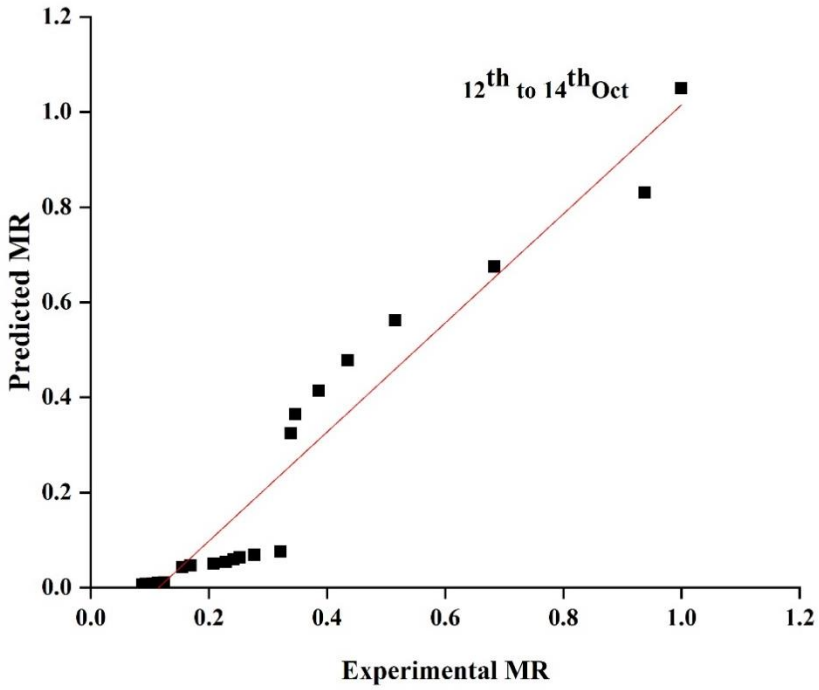

Figure 3.23 Comparison of predicted and experimental MR for OSD of GP by Two Term model for the first batch.

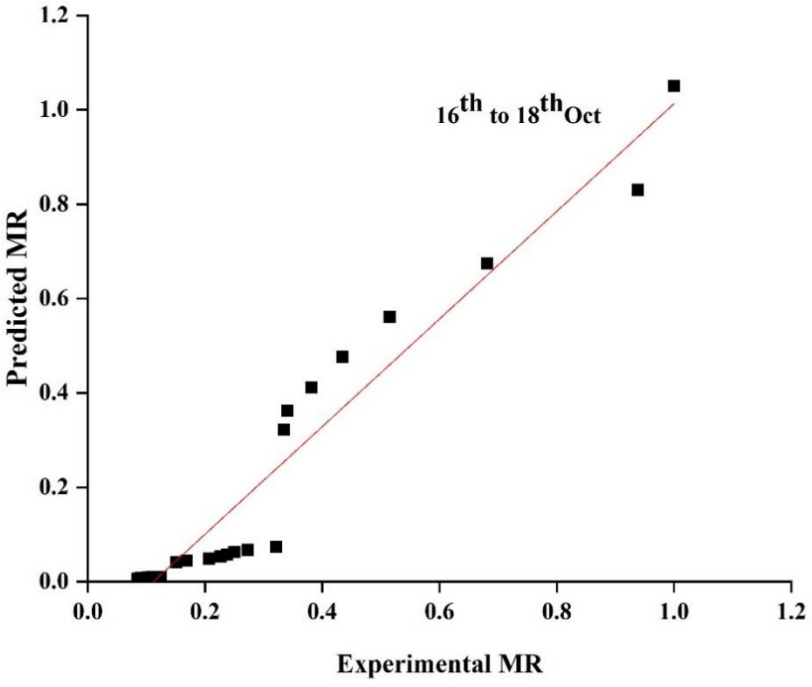

Figure 3.24 Comparison of predicted and experimental MR for OSD of GP by Two Term model for the second batch.

3.7.3 Economic analysis of GP

Processing of a product and its economic growths are inter-linked. The development of a product facilitates people with socio-economic, cultural, and technological evolvement. The economic analysis is carried out with a blend of two methods namely life savings and payback period methods. With a capital cost of FCCSD is $ 93.34, the annual saving was estimated $ 252.99. Table 3.7 gives the cost (approximate) for different components of the FCCSD. For a lifespan of 10 years, the payback period of the FCCSD was estimated as 0.6 year. The production rate of FCCSD is 0.85 kg per batch and the payback period is attractive. The FCCSD was development in-house and some low-cost materials like saw dust/air gap, ply board insulators were used for reduction of thermal losses. Lakshmi et al [109] observed similar payback period for solar drying.

Table 3.7 Economic analysis of FCCSD for GP.

Sl No.	Items	Parameters
1.	Price of the development of the dryer in $	$ 93.34
2.	Predicted lifespan of the dryer	10 years
3.	Price of fresh GP in $	$ 0.40 per kg
4.	Interest rate	10 %
5.	Inflation rate	4.62 %
6.	Annualized capital price in $	$ 14.95
7.	Maintenance price in $	$ 1.49
8.	Salvage value in $	$ 9.34
9.	Annual salvage value in $	$ 0.59
10.	Annualized price in $	$ 15.86
11.	Price of dried GP available in market in $	$ 5.34 per kg
12.	Savings in $	$ 1.68 per day
13.	First-year annual savings in $	$ 253.24
14.	Payback period	0.60 year

Figure 3.25, Figure 3.26 and Figure 3.27 gives the photograph of the same GP which is freshly harvested, in FCCSD and in OSD respectively. It can be stated after observing that FCCSD gives a uniform drying in solar dryer than OSD.

Figure 3.25 Freshly harvested GP

Figure 3.26 GP dried in FCCSD

Figure 3.27 GP dried in OSD

3.8 Summary

The thin layer drying kinetics studies of GP dried under the open sun as well as in free convection corrugated type of solar dryer (FCCSD) with a mathematical modelling was performed. The payback period of the developed dryer was also estimated.

The important conclusions that can be drawn from the analysis are listed below.

- The temperature and relative humidity of the ambient varied within the range of 29.5 °C to 33.8 °C and 61.7 % to 82.3 % respectively for the first batch and 29.2 °C to 34.3 °C and 64.7 % to 80.6 % respectively for the second batch. The inlet and outlet temperature along with relative humidity of FCCSD were recorded for both the batches.
- The average useful heat gain of the integrated solar air heater for the first and second batch was found to be 289.31 W and 290.36 W respectively and the average thermal efficiency was found to be 33.29 % and 33.33 % respectively for the first and second batch.
- The model reported by Midilli and Kucuk was found to be the best model for FCCSD and Two Term model for OSD for both the batches. It took 28 h in FCCSD to reduce the MC from an initial 88 % (w.b.) to 7.22 % (w.b.) for the first batch and 7.1 % (w.b.) for the second batch. But the final MC of 10.18 % (w.b.) and 10.08 % (w.b.) for the first and second batch respectively in OSD of GP was reached in 55 h.

- The average thermal efficiency of the dryer was found to be 10.69 % for the first batch and 10.77 % for the second batch with average specific energy consumption of 68.00 $kWhkg^{-1}$ and 65.54 $kWhkg^{-1}$ for the first and second batch respectively that depended on the time required for drying, product type, and the loading capacity of the dryer.
- The viability of FCCSD to be used commercially for different agricultural products depends upon the economic analysis. The annual savings was estimated to be $ 253.24 with the cost of the construction of the dryer to be $ 93.34.
- The payback period was estimated 0.6 year from the economic investigation of the FCCSD. It is an indication of possible commercialization of the developed dryer for the prospective farmers.
- The FCCSD production capacity was estimated 0.850 kg, per batch. The solar dryer unit may be scaled up to enhance total production rate of FCCSD in future.